European Journal of Phycology

ISSN: 0967-0262 (Print) 1469-4433 (Online) Journal homepage: http://www.tandfonline.com/loi/tejp20

Amphidoma parvula (Amphidomataceae), a new planktonic dinophyte from the Argentine Sea

Urban Tillmann, Marc Gottschling, Valeria Guinder & Bernd Krock

To cite this article: Urban Tillmann, Marc Gottschling, Valeria Guinder & Bernd Krock (2018) Amphidoma parvula (Amphidomataceae), a new planktonic dinophyte from the Argentine Sea, European Journal of Phycology, 53:1, 14-28, DOI: 10.1080/09670262.2017.1346205

To link to this article: https://doi.org/10.1080/09670262.2017.1346205

EUROPEAN JOURNAL OF PHYCOLOGY, 2018
VOL. 53, NO. 1, 14–28
https://doi.org/10.1080/09670262.2017.1346205

Amphidoma parvula (Amphidomataceae), a new planktonic dinophyte from the Argentine Sea

Urban Tillmann[a], Marc Gottschling [b], Valeria Guinder[c] and Bernd Krock[a]

[a]Alfred-Wegener-Institut Helmholtz-Zentrum für Polar- und Meeresforschung, Am Handelshafen 12, D-27570 Bremerhaven, Germany; [b]Department Biologie, Systematische Botanik und Mykologie, GeoBio-Center, Ludwig-Maximilians-Universität München, Menzinger Str. 67, D-80638 München, Germany; [c]Instituto Argentino de Oceanografía, Biogeoquímica Marina, IADO – CONICET, La Carrindanga km 7.5 c.c. 804, B8000FWB Bahía Blanca, Argentina

ABSTRACT

Amphidoma is an old though poorly studied thecate dinophyte that has attracted attention recently as a potential producer of azaspiracids (AZA), a group of lipophilic phycotoxins. A new species, *Amphidoma parvula*, sp. nov. is described from the South Atlantic shelf of Argentina. With a Kofoidean thecal plate pattern Po, cp, X, 6′, 6″, 6C, 5S, 6‴, 2⁗, the cultivated strain H-1E9 (from which the type material of *Am. parvula*, sp. nov. was prepared) shared the characteristic plate arrangement of *Amphidoma* each with six apical, precingular and postcingular plates. *Amphidoma parvula*, sp. nov. differs from other species of *Amphidoma* by a characteristic combination of small size (10.7–13.6 µm in length), ovoid shape, high length ratio between epitheca and hypotheca, and small length ratio between apical and precingular plates. Other morphological details, such as the number and arrangement of sulcal plates and the fine structure of the apical pore complex support the close relationship between *Amphidoma* and the other known genus of Amphidomataceae, *Azadinium*. However, *Am. parvula*, sp. nov. lacks a ventral pore, a characteristically structured pore found in all contemporary electron microscopy studies of *Amphidoma* and *Azadinium*. As inferred from liquid chromatography coupled with tandem mass spectrometry, *Am. parvula*, sp. nov. did not produce AZA in measurable amounts. Molecular phylogenetics confirmed the systematic placement of *Am. parvula*, sp. nov. in *Amphidoma* (as sister species of *Amphidoma languida*) and the Amphidomataceae. The results of this study have improved the knowledge of Amphidomataceae biodiversity.

ARTICLE HISTORY Received 22 February 2017; Revised 9 May 2017; Accepted 18 May 2017

KEY WORDS Argentina; biodiversity; microalgae; new species; phycology

Introduction

Currently, *Amphidoma* F. Stein (Amphidomataceae) encompasses nine marine planktonic dinophyte species. It is an old genus name which was erected by Stein in 1883 as part of his seminal work 'Der Organismus der Infusionthiere'. Stein (1883) described two species new to science within *Amphidoma*, of which Loeblich & Loeblich (1966) chose *Amphidoma acuminata* F.Stein as the type species (the other being the better known species *Amphidoma nucula* F.Stein). The next oldest species initially assigned to *Amphidoma, Am. biconica* Kofoid (Kofoid, 1907*a*), is currently considered a species of *Oxytoxum* F.Stein (Dodge & Saunders, 1985). *Murrayella spinosa* Kofoid was transferred to *Amphidoma* (Kofoid & Michener, 1911) but following reinvestigation by Balech (1971), it has been regarded as a heterotypic synonym of *Am. nucula*. Kofoid & Michener (1911) added five new *Amphidoma* species, namely *Am. curtata* Kofoid & J.R.Michener, *Am. depressa* Kofoid & J.R.Michener, *Am. elongata* Kofoid & J.R.Michener, *Am. laticincta* Kofoid & J.R.Michener and *Am. obtusa* Kofoid & J.R. Michener, with fairly detailed descriptions though lacking illustrations, which makes their identity difficult to infer. Schiller (1929) described *Am. steinii* J. Schiller from the coast of the Mediterranean Sea off Tunisia (with minute illustrations) and Halldal (1953) described *Amphidoma caudata* Halldal from the North Sea off Norway (with outline drawing only).

Until recently, species of *Amphidoma* were scarcely examined. Exceptions are the studies of Balech (1971) and Dodge & Saunders (1985), who all confirmed the plate pattern of *Amphidoma* as having 6′, 0a, 6″, 6C, 6‴, 1p, 1⁗ (initially worked out by Schiller, 1937). Dodge & Saunders (1985) conducted a scanning electron microscopy (SEM) study of *Am. nucula*, and also described the plate pattern of *Am. caudata* for the first time. They showed that the organization of epithecal plates differs significantly in *Am. caudata* from that of other *Amphidoma* species, but they proposed 'that for the present *Am. caudata* should remain in *Amphidoma*' based on the similarity regarding hypothecal plates. They consequently emended the generic diagnosis of *Amphidoma* in order to include *Am. caudata* (Dodge & Saunders, 1985).

CONTACT Urban Tillmann urban.tillmann@awi.de

Published online 01 Nov 2017

In 2009, generic circumscriptions and delimitations were again challenged when Tillmann *et al.* (2009) introduced the genus *Azadinium* Elbrächter & Tillmann. Its type species, *Azadinium spinosum* Elbrächter & Tillmann, was identified as a primary source of azaspiracids (AZAs), a group of lipophilic marine biotoxins associated with human incidents of shellfish poisoning. Later, it became clear that *Am. caudata* has the same plate pattern as *Az. spinosum* and was thus transferred from *Amphidoma* to *Azadinium* (Tillmann *et al.*, 2011; Nézan *et al.*, 2012). Based on morphological and molecular data for a new species of *Amphidoma, Am. languida* Tillmann, R.Salas & Elbrächter, we now know about the sister group relationship between *Azadinium* and *Amphidoma* (Tillmann *et al.*, 2012). Number and arrangement of cingular, sulcal and hypothecal plates, and the characteristic apical pore complex (APC) with a small X-plate centrally invading the first apical plate are morphological similarities and putative synapomorphies between *Amphidoma* and *Azadinium*. These taxa can be distinguished because of six apical but no intercalary plate(s) in *Amphidoma*, and four apical and three epithecal intercalary plates in *Azadinium*.

Amphidoma languida from Ireland produces AZAs that are structurally different from previously reported analogues – they have a modification of the nitrogen-containing I-ring of the molecule (Krock *et al.*, 2012). The discovery of AZA production in *Am. languida* gave rise to renewed interest in *Amphidoma* and subsequently, more strains of *Am. languida* were obtained and investigated. The toxin profile appeared consistent in *Am. languida* and comprised AZA-38 and -39 (Krock *et al.*, 2012), found in the Irish strain (representing the type material), as well as in a strain from Icelandic waters (Tillmann *et al.*, 2015). However, another strain of *Am. languida* was isolated during a period of AZA levels exceeding the EU regulatory limit in different shellfish species on the Atlantic coast of southern Spain. This strain exhibits a different toxin profile consisting of AZA-2 and -43 (Tillmann *et al.*, 2017*b*).

Based on the evidence that has been gathered over the past few years *Am. languida* is now on the list of Harmful Algae (http://www.marinespecies.org/hab/aphia.php?p=taxdetails&id=729889). This has raised interest in other species of *Amphidoma*, which have not been analysed yet for the presence of AZAs. Since the 1990s, the western South Atlantic has been known for dense spring blooms of *Azadinium* (Akselman & Negri, 2012; Akselman *et al.*, 2014), and a retrospective study has shown that the 1992 spring community was very diverse and comprised a number of different species assigned to *Amphidoma* and *Azadinium* (Tillmann & Akselman, 2016). In September 2015 (i.e. Austral spring), we participated in a cruise to the 'El Rincón' area, a coastal sector < 50 m depth, between 38°30′S and 41°30′S in the Argentine Sea, which was extended offshore to sample the Argentinean shelf (~100 m depth). Based on material isolated from the plankton community we here describe a new species of *Amphidoma*, which is characterized morphologically, molecularly and toxinologically.

Materials and methods

Field sampling and cell isolation

A number of clonal strains of Amphidomataceae were established from surface water samples (salinity: 33.6, surface temperature: 7.3°C) collected at the two outer stations, 33 and 34, on the Argentine shelf (Fig. 1). Material was collected during a cruise to the El Rincón area aboard the research vessel *Bernardo Houssay* in September 2015.

Single cells were isolated by micropipetting under a stereomicroscope (M5A, Wild, Heerbrugg, Switzerland). Single cells were transferred into individual wells of 96-well tissue culture plates (TPP, Trasadingen, Switzerland) each containing 250 µl of K-medium (Keller *et al.*, 1987) prepared from 0.2 µm sterile-filtered natural Antarctic seawater diluted 1:10 with filtered seawater from the sampling location. Plates were incubated at 15°C under dim light (*c.* 30 µmol photons m^{-2} s^{-1}) in a controlled environment growth chamber (Model MIR 252, Sanyo Biomedical, Wood Dale, USA). After 3–4 weeks, precursor strains were transferred to 24-well tissue culture plates, each well containing 2 ml of K-medium diluted 1:5 with Antarctic seawater. Exponentially growing strains were finally used as inoculum for batch cultures in 65 ml polystyrene cell culture flasks. A number of successfully established strains of the genus *Azadinium* will be reported elsewhere. One of the strains from station 34 was provisionally labelled H-1E9 and was identified as representing a new species of the genus *Amphidoma*. It was maintained at 15°C under a photon irradiance of 30–50 µmol photons m^{-2} s^{-1} on a 16:8 h light:dark photocycle in a temperature-controlled growth chamber for subsequent detailed microscopic analyses, DNA extraction and toxin analysis.

Microscopy

Observation of living or fixed (formalin: 1% final concentration; or neutral Lugol-fixed: 1% final concentration) cells was carried out using an inverted microscope (Axiovert 200M, Zeiss, Germany) and a compound microscope (Axiovert 2, Zeiss), both equipped with epifluorescence and differential interference contrast optics. The shape and location of the

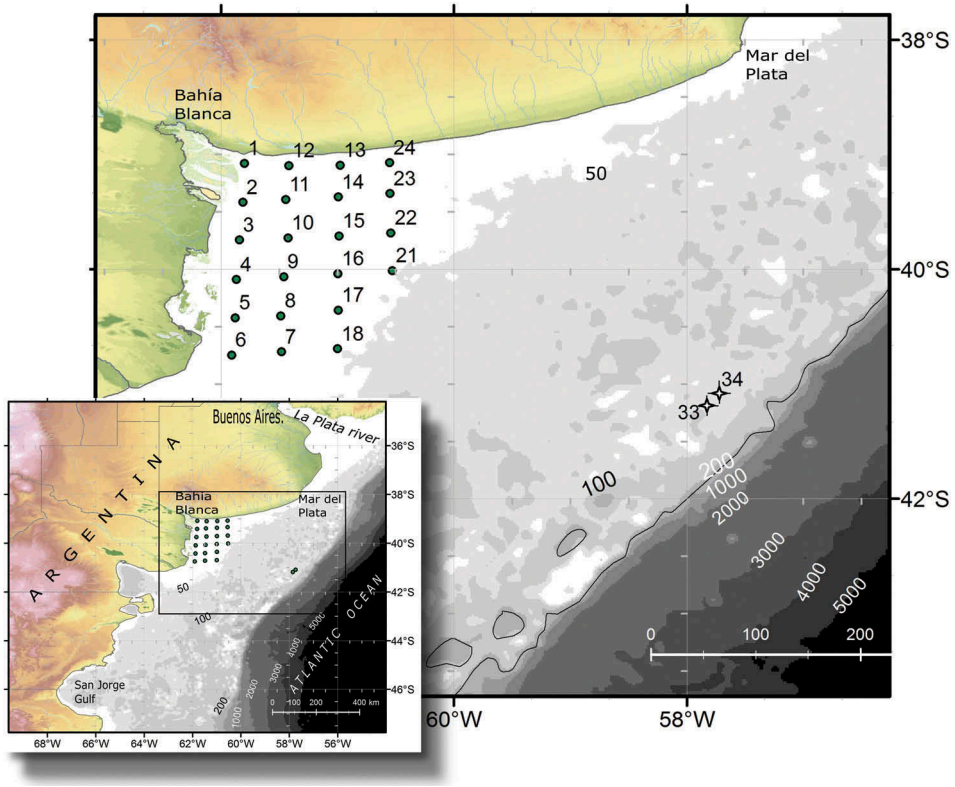

Fig. 1. Study area and location of sampling sites used for cell isolation along the Argentinean coast.

nucleus were determined after staining of formalin-fixed cells with 4'-6-diamidino-2-phenylindole (DAPI, 0.1 µg ml^{-1} final concentration) for 10 min. Photographs were taken with a digital camera (Axiocam MRc5, Zeiss).

Cell length and width of freshly fixed cells (formaldehyde, final concentration 1%) from dense, healthy and growing cultures (based on stereomicroscopic inspection) at late exponential phase were measured at ×1000 using Zeiss Axiovision software (Zeiss). For scanning electron microscopy (SEM), cells were collected by centrifugation (Eppendorf 5810R, 3220 g for 10 min) from 30–50 ml of cell suspension, depending on cell density. The supernatant was removed and the cell pellet resuspended in 60% ethanol in a 2 ml microtube at 4°C for 1 h to strip off the outer cell membrane. Subsequently, cells were pelleted by centrifugation (Eppendorf 5415 R, 16 000 g, 5 min) and resuspended in a 60:40 mixture of deionized water and seawater at 4°C for 30 min. After centrifugation and removal of the diluted seawater supernatant, cells were fixed with formaldehyde (2% final concentration in a 60:40 mixture of deionized water and seawater) and stored at 4°C for 3 h. Cells were then collected on polycarbonate filters (Millipore, 25mm Ø, 3 mm pore-size) in a filter funnel, in which all subsequent washing and dehydration steps were carried out. A total of eight washings (2 ml MilliQ-deionized water each) were followed by a dehydration series in ethanol (30, 50, 70, 80, 95, 100%; 10 min each). Filters were dehydrated with hexamethyldisilazane (HMDS), first in 1:1 HMDS:EtOH followed by twice 100% HMDS, and then stored under gentle vacuum in a desiccator. Finally, filters were mounted on stubs, sputter coated (Emscope SC500, Ashford, UK) with gold-palladium and viewed under a SEM (FEI Quanta FEG 200, Eindhoven, the Netherlands). Micrographs were presented on a black background using Adobe Photoshop 6.0 (Adobe Systems, San Jose, USA).

Molecular phylogeny

For DNA extraction of strain H-1E9, 50 ml of healthy and growing suspension (based on stereomicroscopic inspection) were harvested by centrifugation (Eppendorf 5810R, Hamburg, Germany; 3220 g for 10 min). The pellet was transferred to a microtube, centrifuged again (Eppendorf 5415, 16 000 g, 5 min) and stored frozen at –80°C until use. DNA isolation, PCR amplification and sequencing followed standard protocols that were described previously (Tillmann *et al.*, 2017*b*). New sequences were added to an existing alignment covering the molecular and morphological diversity known from Amphidomataceae, and phylogenetic analyses were run in the same way as described previously (Tillmann *et al.*, 2014*a*).

Chemical analysis of azaspiracids

For toxin analysis, strain H-1E9 was grown in 250 ml plastic culture flasks. For each harvest, cell density was determined by settling Lugol-fixed samples and counting > 800 cells under an inverted microscope. Cells were harvested at cell densities of about 2–8 × 10^3 cells ml^{-1} in four 50-ml centrifugation tubes. After centrifugation (Eppendorf 5810R) at 3220 g for 10 min, the four pellets were pooled in a microtube, centrifuged again (Eppendorf 5415, 16 000 g, 5 min) and stored at −20 °C until use. Growth and harvest procedures were repeated several times to yield a total number of 23.3 × 10^6 cells. All harvests were combined in 2 ml methanol and homogenized with a sonotrode (Sonoplus HD 2070, Bandelin) for 70 cycles at 100% power for 70 s. Homogenates were centrifuged (Eppendorf 5810 R, 15°C, 3220 × g, 15 min). Supernatants were collected and pellets twice re-extracts with 1 ml methanol each. Combined extracts were reduced in a rotary evaporator (Büchi) at reduced pressure and 40°C in a water bath to a volume < 0.5 ml and were then taken up in acetone to a final volume of 0.5 ml. The extracts were transferred to a 0.45 µm pore-size spin-filter (Millipore) and centrifuged (Eppendorf 5415 R, 800 × g, 30 s), with the resulting filtrate transferred into a liquid chromatography (LC) autosampler vial for LC-MS/MS analysis.

The sample was tested for a wide array of AZAs, including those which are currently known to be produced by dinophytes, by tandem mass spectrometry in the selected reaction monitoring (SRM) mode as described in detail by Tillmann *et al.* (2017*a*). All transitions for this experiment are given in Table 1. In addition, precursor ion scans of the typical AZA fragments *m/z* 348, 360 and 362 were performed (Tillmann *et al.*, 2017*a*) in order to detect possible unknown variants.

Table 1. Mass transitions m/z (Q1>Q3 mass) and their respective AZAs.

Mass transition	Toxin	Collision energy (CE) [V]
716>698	AZA-33	40
816>798	AZA-39	40
816>348	AZA-39	70
828>658	AZA-3	70
828>810	AZA-3, AZA-43	40
830>812	AZA-38	40
830>348	AZA-38	70
842>672	AZA-1	70
842>824	AZA-1, AZA-40	40
844>826	AZA-4, AZA-5	40
846>828	AZA-37	40
856>672	AZA-2	70
856>838	AZA-2	40
858>840	AZA-7, AZA-8, AZA-9, AZA-10, AZA-36	40
868>362	AZA-55	70
870>852	Me-AZA-2	40
872>854	AZA-11, AZA-12	40

Results

Amphidoma parvula Tillmann & Gottschling sp. nov. (Figs 2–44)

Description: Small photosynthetic thecate Dinophyceae; cells 10.7–13.8 µm long and 9.6–12.9 µm wide; one large pyrenoid laterally positioned on the left lateral side of the cell; cingulum broad (*c.* 30% of cell length) and postmedian; hypotheca flat and narrower than epitheca, tabulation formula: Po, cp, X, 6′, 0a, 6″, 6C, 5S, 6‴, 2⁗; precingular plates about twice as long as apical plates; ventral pore absent.

Holotype: SEM-stub prepared from clonal strain H-1E9 (designated CEDiT2017H63), deposited at the Senckenberg Research Institute and Natural History Museum, Centre of Excellence for Dinophyte Taxonomy (Germany).

Isotypes: Formalin fixed sample prepared from clonal strain H-1E9 (designated CEDiT2017I64) deposited at the Senckenberg Research Institute and Natural History Museum, Centre of Excellence for Dinophyte Taxonomy (Germany)

Type locality: South Atlantic Ocean, off Argentina (41°5.6′S, 57°43.2′W).

Habitat: Marine plankton.

Strain establishment: Sampled by U. Tillmann on 9 September 2015, isolated by U. Tillmann on 18 September 2015.

Etymology: The epithet (Lat. *parvulus* – small) is inspired by the conspicuously small size of the species.

Light microscopy (LM)

Motile cells of strain H-1E9 regularly concentrated at the bottom of the culture vessel. They exhibited a conspicuous swimming behaviour in that they mostly moved very slowly but occasionally performed sudden jumps. These jumps generally occurred when cells approached the bottom of the culture vessel (see Supplementary video).

Cells of *Am. parvula*, sp. nov. were mushroom-shaped, with a dome-shaped episome terminating in a distinctly acuminate apical pore (Figs 2–6). Cells were small with a median length of 12.1 µm (10.7–13.6 µm, n = 57) and a median width of 11.0 µm (9.6–12.9 µm, n = 57). The episome was slightly wider and distinctly longer than the irregularly flattened hyposome, so that the broad cingulum was postmedian in position (Figs 2–6).

A single large, lobed and reticulate chloroplast expanded through the entire cell (Figs 2–7) with one large pyrenoid laterally positioned on the left lateral side of the cell in the cingular plane (Figs 2, 4, 6, 8). Occasionally, a globose structure (putatively a

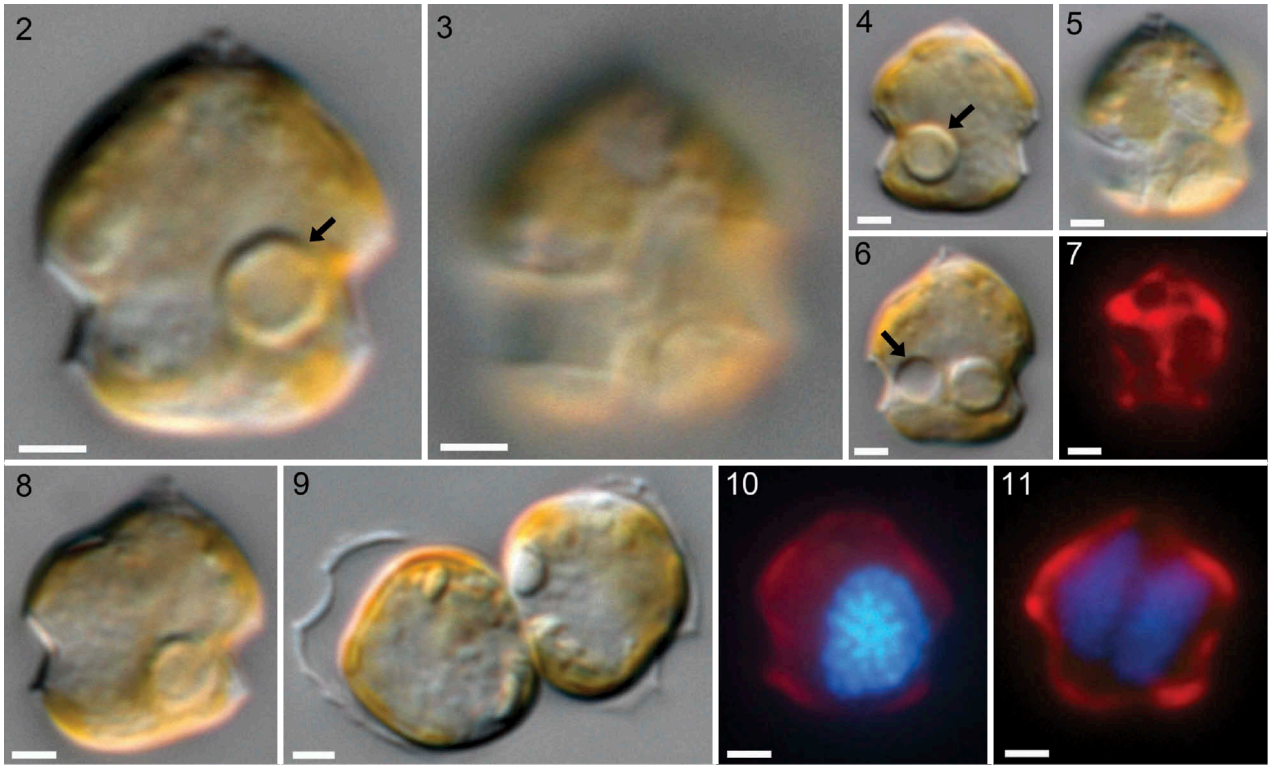

Figs 2–11. *Amphidoma parvula*, sp. nov. (strain H-1E9): LM of living and formalin fixed cells. **Figs 2–6**. Living cells in ventral (Figs 2, 3, 5, 6) or dorsal view (Fig. 4) showing general size and shape. Note the presence of a large pyrenoid in the cingular plane (arrow in Figs 2, 4). Figs 2, 3. Two focal planes of the same cell (ventral view) showing that the pyrenoid is located on the cell's left side. Fig. 6. A round putative pusule (arrow) located next to the pyrenoid. **Fig. 7.** Epifluorescence view of formalin fixed cells; chlorophyll autofluorescence to show the chloroplast structure. **Figs 8, 9.** Living cells, presumably in early (Fig. 8) and late (Fig. 9) stage of cell division. **Figs 10, 11.** Epifluorescence view (UV excitation) of formalin fixed and DAPI stained cells, note the elongated and longitudinally divided nucleus in Fig. 11. Scale = 2 µm.

pusule) adjacent to the pyrenoid was visible (Fig. 6). The large, ellipsoid nucleus was positioned in the centre of the cell on the right lateral side (Figs 4, 10). Before cell division, cells mainly increased in width (Fig. 8) and during division, the nucleus first elongated and then started to divide (Fig. 11). Cytokinesis occurred in motile cells and was of the desmoschisis type, where the parental theca was shared between the two sister cells (Fig. 9).

Scanning electron microscopy (SEM)

Thecal plates of cells were thin, but could be clearly observed in light microscopy (Fig. 9), and were stainable with calcofluor white (not shown). However, the Kofoidean pattern was better resolved by SEM due to the delicacy of the plates (Figs 12–40). The plate formula was Po, cp, X, 6′, 0a, 6″, 6C, 5S, 6‴, 2⁗ and is schematically drawn in Figs 41–44. Plates were generally smooth, but growth bands were faintly visible occasionally as striated rows running parallel to plate sutures (e.g. Figs 13, 18). The presence of these growth bands was restricted to particular sutures.

The acuminate epitheca terminated in the prominent apical pore complex (APC) (Figs 12–14, 16–18, 20–23) composed of three plates: a pore plate (Po) covered by a cover plate (cp) and the canal plate X (Figs 22, 23). The pore plate was teardrop-shaped and was confined by a raised collar formed by the edges of the apical plates. On the tapered ventral side of the pore plate, the collar was open but could be extended to trace the sutures between plate 1′ and its two joining apical pates 2′ and 6′ (e.g. Fig. 16). In the centre of the apical pore plate (Po), a round to teardrop-shaped pore emerged which was covered by a cover plate (cp). A small X-plate was located where the pore plate abutted the first apical plate. The dimension and shape of the X-plate was visible when seen from the cell's interior view (Fig. 24). It was small, occupying about 1/2 of the connection between the pore and 1′, and tongue-like in shape. From the exterior, the X-plate had a very characteristic three dimensional structure with finger-like protrusions contacting the apical cover plate (Figs 22, 23). In addition to the APC, the epitheca was composed of 12 thecal plates (Figs 17, 18, 20, 21) forming rows of six apical and six precingular plates. Epithecal intercalary plates were absent (Figs 17, 18). On the epitheca, the ratio of apical plate length to precingular plate length was typically

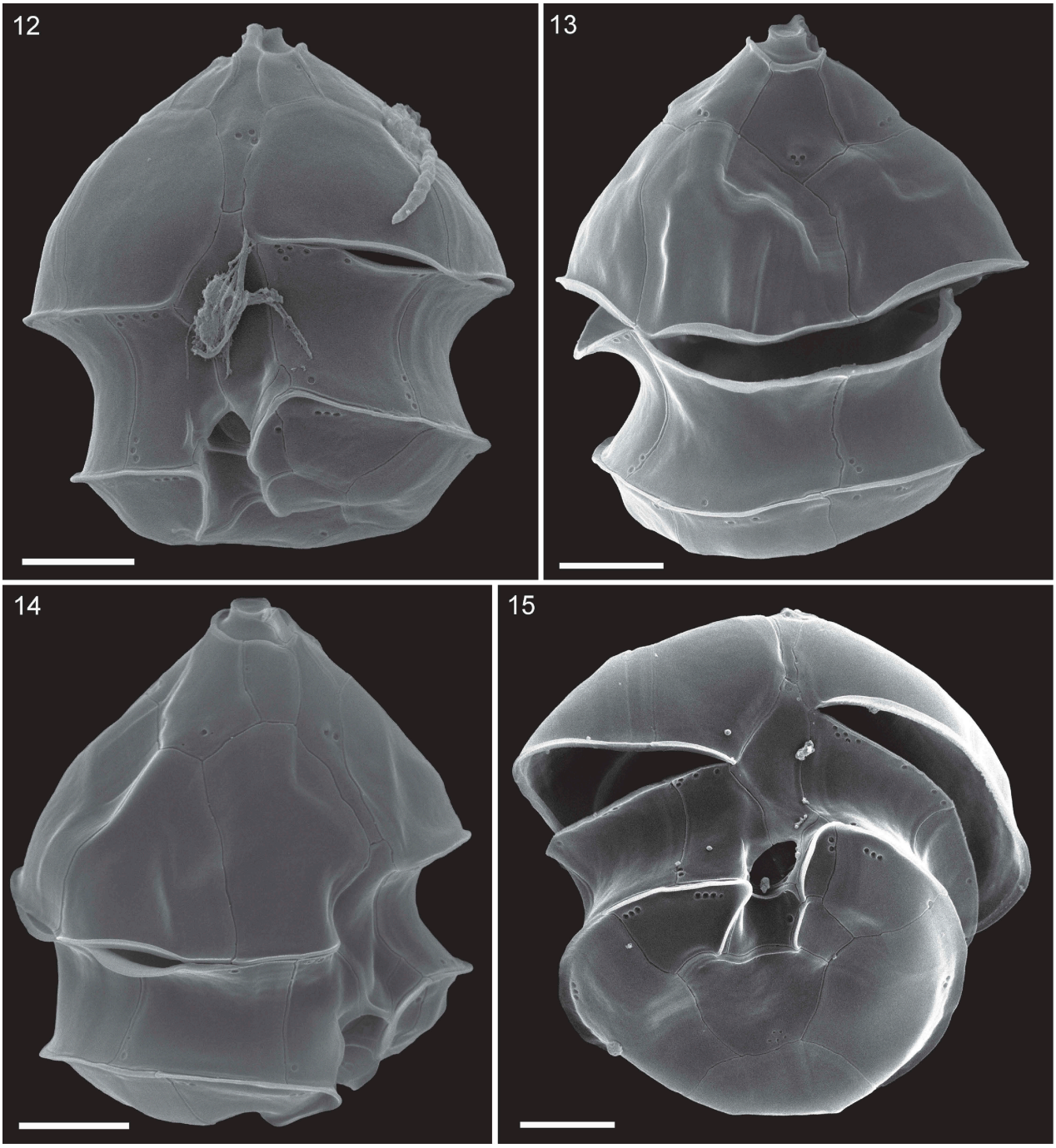

Figs 12–15. *Amphidoma parvula*, sp. nov. (strain H-1E9): SEM micrographs of different cells. **Fig. 12.** Ventral view. **Fig. 13.** Dorsal view. **Fig. 14.** Right-lateral view. **Fig. 15.** Antapical-ventral view. Scale = 2 µm.

about 1:2. The first apical plate was diamond-shaped in its anterior part and narrowed in its posterior part (Figs 12, 16, 17). The ventral apical plates 2′ and 6′ were small, typically of equal size, and had a curved right or left side, respectively (Figs 16–18). The lateral apical plates 3′ and 5′ were hexagonal and larger in size than the ventral apical plates (Figs 17, 18, 20, 21). The dorsal apical plate 4′ was quadrangular and lanceolate (Figs 13, 18, 20). All six precingular plates were large and of comparable size (Figs 18, 20, 21).

The hypotheca was composed of six postcingular and two antapical plates (Figs 16, 17). The first postcingular plate 1‴ was minute, almost rectangular and had a length/width ratio > 2, with the curved left side bearing the sulcal/cingular list. Plates 2‴, 4‴ and 6‴ were of comparable size, whereas the lateral postcingular plates 3‴ and 5‴ were slightly larger. Plate 3‴ was in contact with both antapical plates. The two antapical plates were distinctly different in size. The small plate 1⁗ was longer than it was wide, positioned laterally to the posterior sulcal plate, was roughly the same width as plate 1‴ and bore the most posterior part of the left sulcal list (Figs 16, 17).

The cingulum was wide, about 1/3 of total cell length, and was displaced by about 1/3 of its width

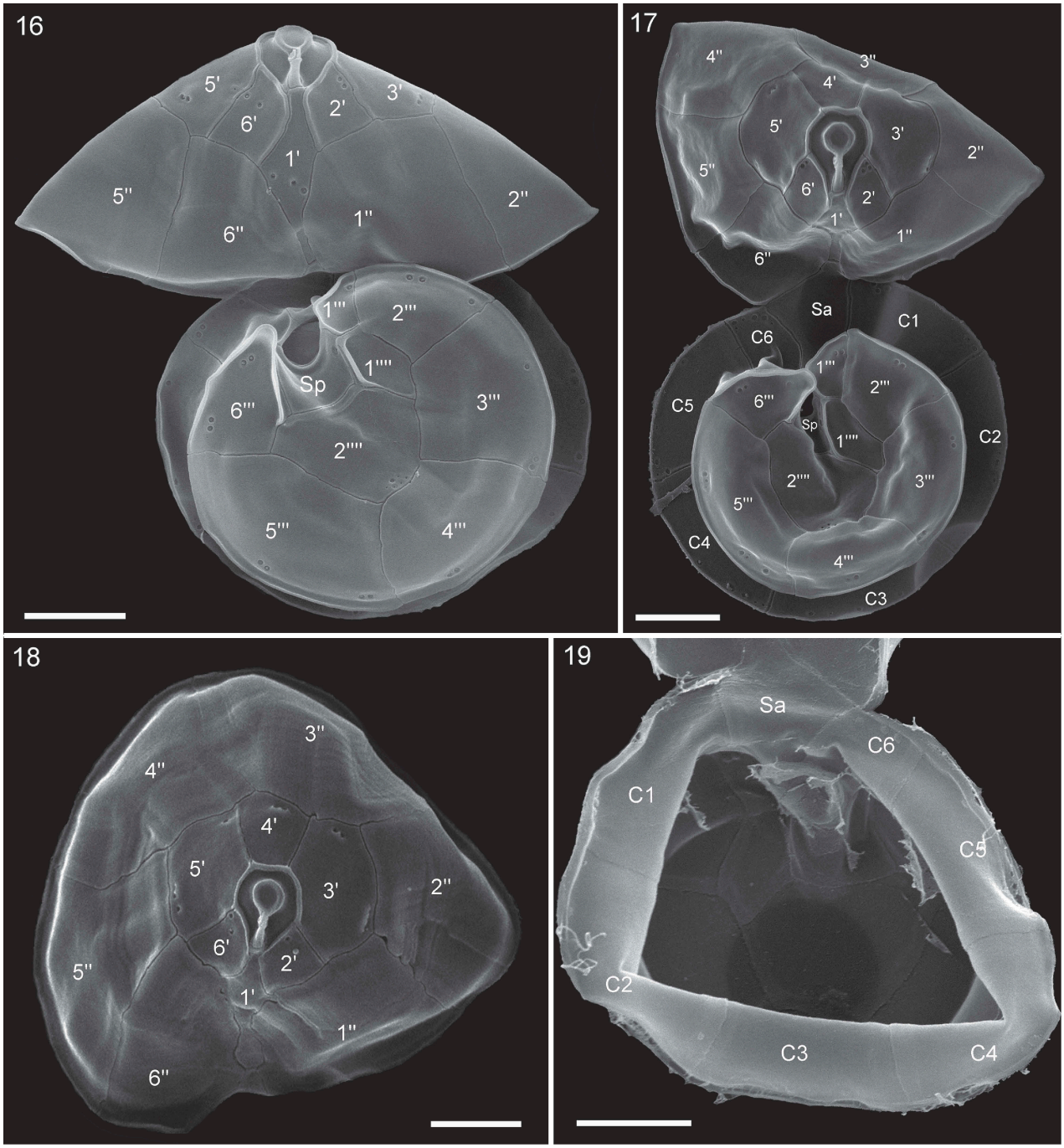

Figs 16–19. *Amphidoma parvula*, sp. nov. (strain H-1E9): SEM micrographs of different cells. **Figs 16, 17.** Unfolded thecae allowing antapical view of the hypotheca and ventral (Fig. 16) or apical (Fig. 17) view of the epitheca. **Fig. 18.** Apical view showing the complete series of epithecal plates. **Fig. 19.** Apical view showing cingular plates. Scale = 2 µm.

(Fig. 12). There were six cingular plates (Figs 17, 19). Five of the cingular plates were of comparable size, but the right cingular plate C6 was distinctly narrower. The sulcus (Figs 12, 15, 25–27) was deeply concave and extended all along the hypotheca. The sulcal plates were difficult to resolve because of the internal vaulted structure of the flagellar pore region. Nevertheless, at least five sulcal plates could be identified (Figs 25–27). The large anterior sulcal plate (Sa) was asymmetrical pentagonal and partly invaded the epitheca (Figs 12, 15, 25). On the anterior tip of plate Sa, a depression with a roundish rim was visible in some of the cells (Figs 28–35), usually positioned at the left upper margin of the Sa plate. As compiled in Figs 28–35 the shape and characteristics of this 'ventral depression' were variable among cells, ranging from distinctly developed through to faintly expressed and in many cases it was either not present or almost indiscernible. Two small plates, namely a median sulcal (Sm) and a right sulcal (Sd) plate, formed the inverted part of the sulcus. A left sulcal plate (Ss) ran horizontally from C1 to C6, thereby separating the posterior sulcal plate (Sp) from the other sulcal plates. In its

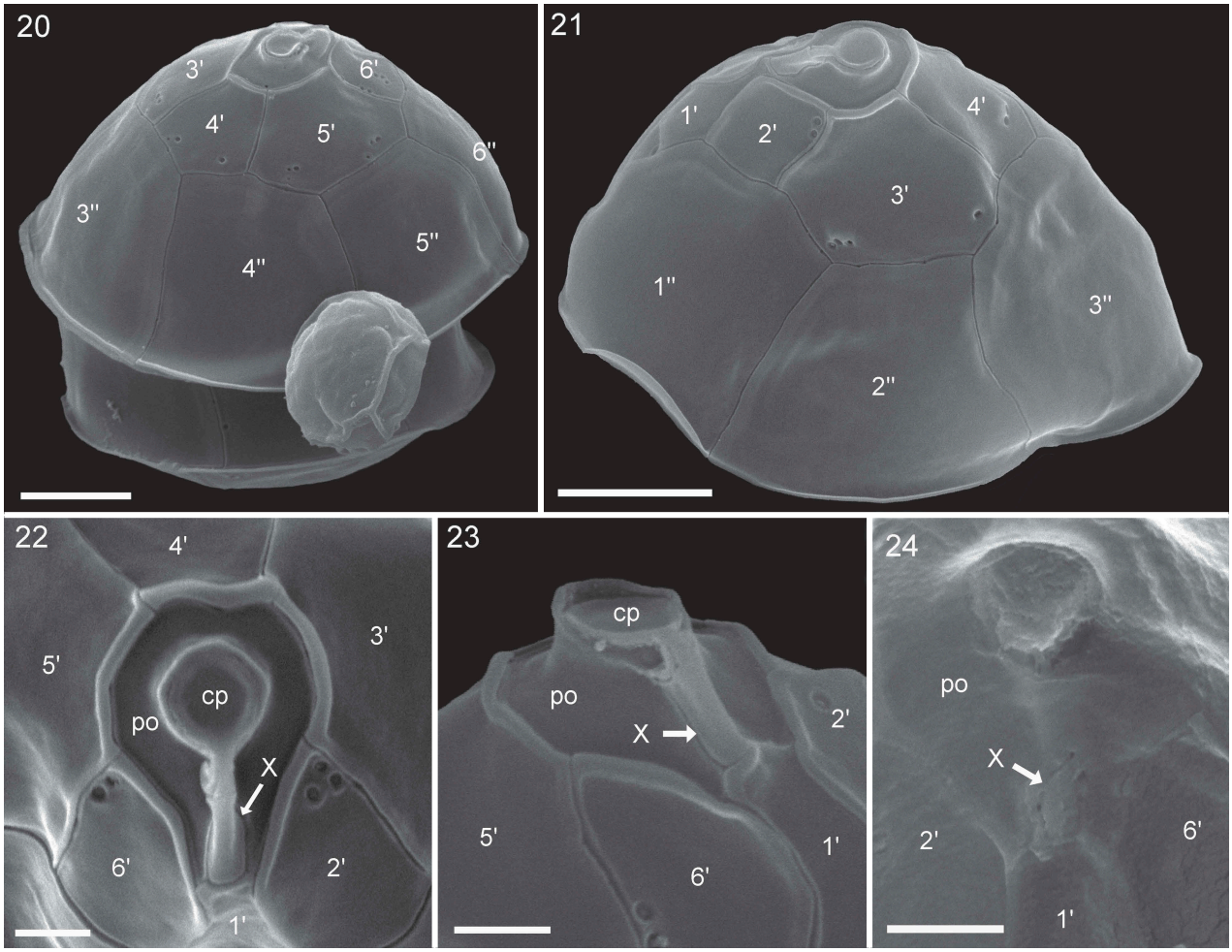

Figs 20–24. *Amphidoma parvula*, sp. nov. (strain H-1E9): SEM micrographs of different cells. **Figs 20, 21**. Epitheca in right-lateral (Fig. 20) and left-lateral (Fig. 21) view. **Figs 22–24.** Details of the apical pore complex (APC). Fig. 24. APC viewed from cell interior. Abbreviations: Po = pore plate; X = X-plate, cp = cover plate. Scale: Figs 20, 21 = 2 µm; Figs 22–24 = 0.5 µm.

median and right part, this plate was very narrow and therefore difficult to resolve and to discern from the parallel running anterior ridge of the Sp plate (Figs 25–27). The posterior sulcal plate was rectangular in shape but deeply concave and was laterally bordered by distinct sulcal lists. A list-like thickening was typically present on plate C6 (Figs 25, 26).

Thecal plates contained a limited number of thecal pores having a diameter of about 0.1 µm (Figs 12–15). As indicated in Figures 41–44, pores were characteristically located on apical, cingular and postcingular plates, whereas all precingular plates were free of pores consistently. On the posterior sulcal plate 1–3 pores were present, whereas the anterior sulcal plate was always free of pores. Among the antapical plates, the small plate 1′′′′ was always free of pores. On the larger plate 2′′′′, a field of pores was present adjacent to the suture with plate 4′′′, and pores were typically arranged in rows. The number of pores on plate 2′′′′ typically was 6–8, but could be quite variable ranging between 2 and 14 (Figs 36–40). In addition, pores were positioned at both anterior and posterior rims of the cingular plates (e.g. Figs 12, 13).

The plate pattern shown in Figures 41–44 was the standard basic pattern. However, a number of variations occurred in the cultures. Most common were aberrations of apical plates varying in size, shape, and number (see Supplementary figs S1–S12). Abnormal patterns of precingular and hypothecal plates were also observed rarely (Supplementary figs S13–S21).

Molecular phylogeny

ITS and LSU sequences were generated and deposited as a new GenBank entry (KY996792) in the course of the study (Supplementary table S1). The SSU+ITS+LSU alignment of the Amphidomataceae was 1841+1321+3561 bp long and comprised 462 +750+867 parsimony informative sites (30.9%, mean of 9.04 per terminal taxon). Fig. 45 shows a cut-off of the best-scoring Maximum Likelihood (ML) tree (–ln=98 802.12) focusing on

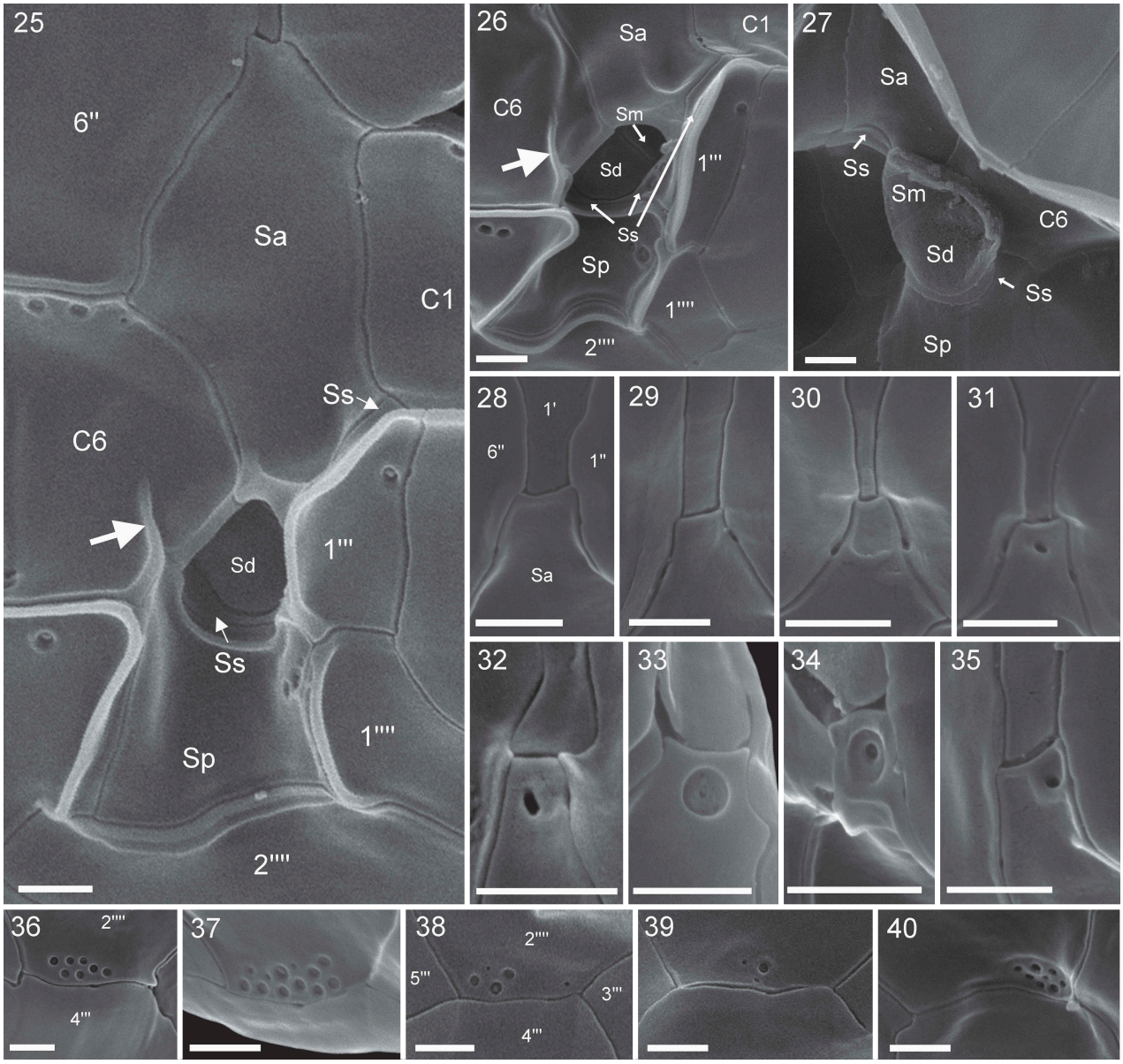

Figs 25–40. *Amphidoma parvula*, sp. nov. (strain H-1E9): SEM micrographs of different cells. **Figs 25–27.** Details of the sulcal plate arrangement in external (Figs 25, 26) and internal (Fig. 27) view. Note the list-like thickening on plate C6 (arrows in Figs 25 and 26). **Figs 28–35.** Detailed view of the anterior sulcal plate Sa showing different appearances of the ventral depression. **Figs 36–40.** Detailed view of the cluster of pores located on plate 2''''. Abbreviations: Sa: anterior sulcal plate; Sp: posterior sulcal plate; Ss: left sulcal plate; Sm: median sulcal plate; Sd: right sulcal plate. Scale = 0.5 µm.

Amphidomataceae, with the internal topology not fully resolved. However, many nodes were statistically well if not maximally supported, and a number of lineages could be distinguished such as *Az. caudatum* (100LBS, 1.00BPP), *Az. concinnum* Tillmann & Nézan (100LBS, 1.00BPP), *Az. cuneatum* Tillmann & Nézan (100LBS, 1.00BPP), *Az. dalianense* Z.Luo, H.Gu & Tillmann (92LBS, 1.00BPP), *Az. dexteroporum* Percopo & Zingone (95LBS, 1.00BPP), *Az. poporum* Tillmann & Elbrächter (75LBS, 0.95BPP), *Az. spinosum* (82LBS, 0.95BPP), *Az. trinitatum* Tillmann & Nézan (100LBS, 1.00BPP) and *Az. zhuanum* Z.Luo, Tillmann & H.Gu (100LBS, 1.00BPP).

Strain H-1E9, from which type material of *Am. parvula*, sp. nov. was prepared, clustered together with a sequence (KT389900) derived from an environmental sample collected in the South China Sea (100LBS, 1.00BPP). Together, they constituted the sister group (100LBS, 1.00BPP) of OTUs being assigned to *Am. languida* (71LBS, 0.96BPP, including some environmental sequences: KJ22-3-61, SCM28C60).

Azaspiracids

Strain H-1E9 was tested for a wide array of AZAs including those which are currently known to be produced by dinophytes as detailed in Table 1.

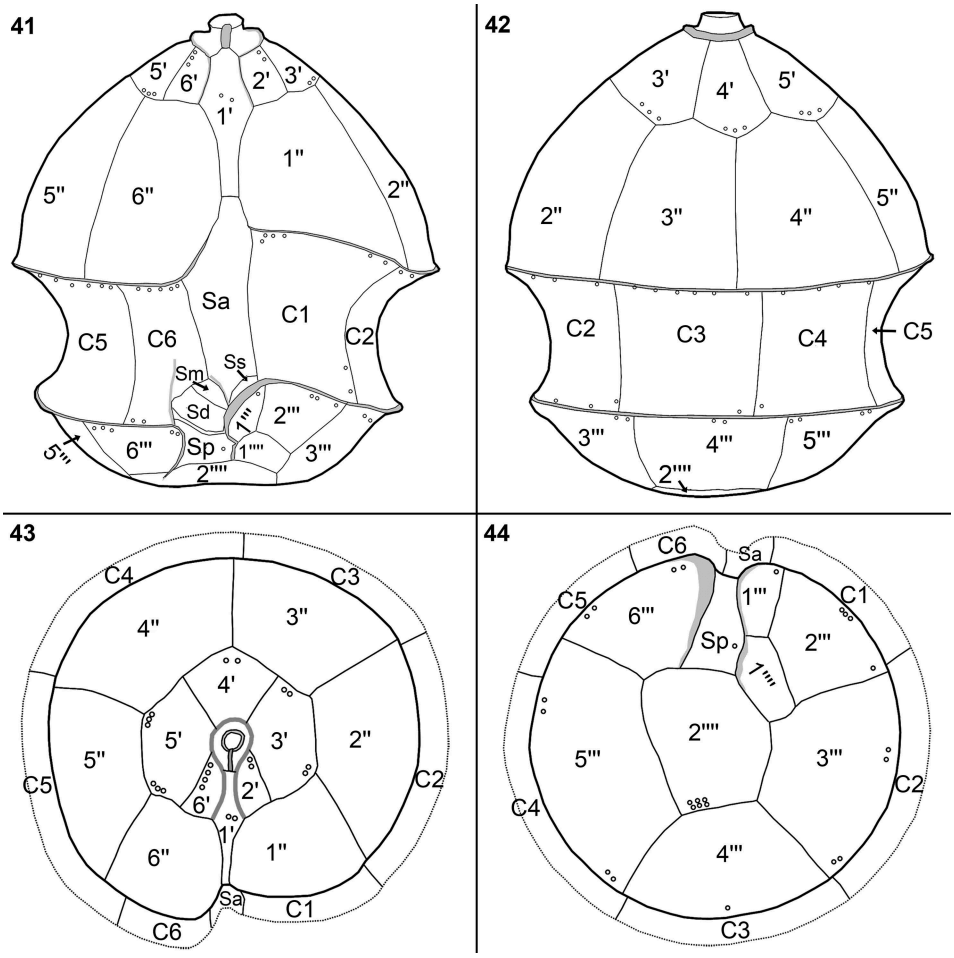

Figs 41–44. *Amphidoma parvula*, sp. nov.: Schematic illustration of thecal plates (as inferred from the investigation of strain H-1E9). **Fig. 41.** Ventral view. **Fig. 42.** Dorsal view. **Fig. 43.** Apical view. **Fig. 44.** Antapical view. Abbreviations: Sa: anterior sulcal plate; Sd: right sulcal plate; Sm: median sulcal plate; Sp: posterior sulcal plate; Ss: left sulcal plate.

None of these AZAs were above the detection limit of 0.006 fg cell^{-1}. In addition, all three precursor ion scans of the typical AZA fragments *m/z* 348, 360 and 362 showed no signals, which excluded the presence of any other AZA-related compounds at cell quotas higher than the detection limit of these experiments of 0.4 fg cell^{-1}.

Discussion

Our complementary approach using morphological and molecular sequencing techniques provides evidence for the distinctiveness of *Am parvula*, sp. nov. and the systematic position of the new species within the Amphidomataceae. Morphologically, the presence of six plates in each of the apical, precingular, cingular and postcingular series, and the lack of anterior intercalary plates, confirm the strain H-1E9 as a new member of *Amphidoma*. The morphological data are corroborated by molecular phylogenetics, in which the monophyly of *Amphidoma* including *Am. parvula*, is not in any doubt. The unique combination of morphological features (Table 2), but also the distinctiveness in the molecular tree, justify the description of *Am. parvula* as a new species.

Cells of strain H-1E9, from which the type material of *Am. parvula*, sp. nov. has been prepared, differ from most other species of *Amphidoma* in shape and size (Table 2). Of the nine previously described species, the majority has a biconical or an elongated cell shape, whereas only three (*Am. curtata, Am. laticinta* and *Am. languida*) share a non-elongated shape with *Am. parvula*, sp. nov. Among those, *Am. laticincta* and *Am. languida* are the only species smaller than 20 µm in length. The mushroom-shaped *Am. parvula*, sp. nov. differs from spheroidal *Am. laticincta* because of its shape, the distinctly greater ratio between epitheca and hypotheca (2 in *Am. parvula*, 1 in *Am. laticinta*) and the apical plates being consistently shorter (*c.* half of the length) than precingular plates. *Amphidoma parvula* further differs from *Am. languida* because of its slightly smaller size, its flat hypotheca and the absence of a ventral pore on plate 1′. In addition, *Am. languida* has a group of pores on the 2′′′′ plate that is arranged within a round rim with the appearance of one large antapical pore,

Fig. 45. Maximum Likelihood (ML) tree (–ln=98,802.12) of 95 Amphidomataceae operational taxonomic units (OTUs), derived from the comparison of concatenated rRNA sequences (cut-off without outgroup i.e. Gymnodiniaceae s.str. and Peridiniales). Branch lengths are drawn to scale, with the scale bar indicating the number of nt substitutions per site. The numbers on the branches are statistical support values (above: ML bootstrap values, values < 50 are not shown; below: Bayesian posterior probabilities, values < 0.90 are not shown). Asterisks indicate maximal support.

whereas the group of pores on the 2'''' plate of *Am. parvula* are not specifically bordered and are arranged in rows. Apical plates of *Am. languida* are distinctly smaller than the precingular plates (apical to precingular length ratio of *c.* 0.2; compared to a ratio of 0.5 in *Am. parvula*).

The putatively apomorphic number of six plates in all of the major plate series underlines the monophyly of *Amphidoma*, but details of more subtle parts of the theca, such as the sulcal region and the APC, are not well known for the majority of species. The detailed segmentation of the sulcal region is often difficult to

Table 2. Morphological features of *Amphidoma* spp. Grey shaded areas highlight features that *Am. parvula* shares with a few other *Amphidoma* species.

	biconical or elongate species						spheroidal ovoid species			
feature	*Am. nucula*	*Am. acuminata*	*Am. steinii*	*Am. obtusa*	*Am. elongata*	*Am. depressa*	*Am. curtata*	*Am. laticincta*	*Am. languida*	*Am. parvula*
length	30.5 – 50[1]	not described	34	27	35 – 40	27	30	18	13.1	12.1
width	21 – 30[1]	not described	30	18	18 – 23	27	23	17	11.9	11.0
length/width ratio	1.6	2.4[2]	1.1	1.4	2	1	1.3	1.05	1.2	1.1
general shape	biconical	acute biconical	broad biconical	acute biconical	elongate	biconical	not biconical	spheroidal	ovoid	mushroom-shaped
ratio epitheca- to hypotheca	1.7	1.2	1.3	1	1	>1 (hypotheca very low)	>1 (epi greatly exceeding hypo)	1	1.5	2
ratio apical to precingular plates	0.25	0.25	0.4	2	2	Not described	0.3	1	0.2	0.5
apex	tapered	acute conoid	blunted or broadly pointed	not described	as *Am. acuminata*, but more obtuse anteriorly	scarcely differentiated apical horn	truncate, displaced to the right	abruptly rounded to small apical closing platelet	pointed, distinct apical pore	dome-shaped, pointed
antapex	short blunt horn	slender, long horn	conical but without horn	broadly rounded	blunt, curved ventrally, without acicular spinule	obtuse median antapical horn	very low dome	hemispherical	hemispherical, slightly pointed, with large antapical pore	flat
shape 1′	slender	not described	slender	asymmetrically diamond-shaped	elongate, diamond-shaped	asymmetrically diamond-shaped	slender	symmetrically diamond-shaped	slender	diamond-shaped
plate 6″	rectangular 1.5 /1	not described	rectangular 1.5. /1	squarish	pentagonal	pentagonal	slender 1 /5	not described	trapezoidal 1 /1.8	trapezoidal 1 /1.8
ventral pore (vp)	at posterior tip of 1′ [3]	not described	not described	not described	right edge of apical 1′	not described	not described	at midventral posterior tip of apical 1′	vp atanterior right side of plate 1′; vd[4] at posterior tip of 1′	no vp; vd at times at anterior tip of plate 1′
shape 1‴	long, spindle shaped	small, squarish[2]	medium, squarish	minute, subtriangular	small, triangular	small rectangular	small, squarish	very minute, nearly rectangular	broad trapezoidal	small, rectangular
cingulum	narrow, ca. 8% of cell length	narrow, ca.8% of cell length	medium, ca. 12% of cell length	very narrow	"as *Am. acuminata*" (narrow)	medium, ca.20% of cell length, not displaced	medium, ca..15% of cell length	broad, not displaced	narrow, ca. 8% of cell length	broad, ca. 30% of cell length
plate surface	reticulate	very delicate	with pores arranged in rows	smooth	smooth	smooth	finely, faintly and regularly reticulate	smooth and structureless	smooth	smooth
other				less elongated than *Am. acuminata*	resembling *Am. acuminata*; antapical 2‴″ asymetrical		1‴″ and 2‴″ about equal in size		plate 2‴″ with antapical pore (depressed field of pores with a broad rim)	plate 2‴″ with a group of pores arranged in rows
reference	Stein (1883), Balech (1971), Kofoid (1907 *b*)	Stein (1883)	Schiller (1937)	Kofoid & Michner (1911)	Kofoid & Michner (1911)	Kofoid & Michner (1911)	Kofoid & Michner (1911)	Kofoid & Michner (1991)	Tillmann *et al.* (2012)	this study

[1]Size taken from Balech (1971). [2]Derived from the figure given in Stein (1883). [3]A vp is depicted for *Am. spinosa* (= *Am. nucula*) in Kofoid (1907*b*). The figure in Kofoid (1907*b*) is labelled with 'vp'. The corresponding description is: 'longitudinal furrow on the epitheca only a narrow groove terminating in a pit". [4]vd = ventral depression.

elaborate for Dinophyceae, and there are only few reports on the number of sulcal plates for other species of *Amphidoma*. In his detailed morphological study of *Am. nucula*, Balech (1971) reported a total of four sulcal plates (i.e. Sa, Ss, Sd, Sp), with the right sulcal plate Sd being tiny and located adjacent to the posterior edge of C6. Despite the clear description of four sulcal plates by Balech (1971), Dodge & Saunders (1985) cited Balech as reporting three sulcal plates and in their study they consequently (though probably wrongly) also listed three sulcal plates. However, they did not provide additional descriptions and/or micrographs of this trait. *Amphidoma parvula* clearly has five sulcal plates in a very characteristic arrangement. Plate Ss runs horizontally from C1 to C6 and forms with two small plates the cavity. The consistent presence of this characteristic arrangement of sulcal plates in *Azadinium* (Tillmann *et al.*, 2014*b*), *Am. languida* (Tillmann *et al.*, 2012) and in *Am. parvula* may argue for a sister group relationship between *Amphidoma* and *Azadinium* and thus the monophyly of the Amphidomataceae. It is predicted from phylogenetic trees that other species of *Amphidoma* may share the same number and arrangement of sulcal plates, but detailed SEM studies of other species of *Amphidoma* are needed for confirmation.

The APC fine structure of *Amphidoma parvula* conforms to that elucidated for *Am. languida* and for all species of *Azadinium* (Tillmann *et al.*, 2012; Tillmann & Akselman, 2016). The presence of the minute X-plate is not mentioned in most of the older literature, but it is noted as a 'diminuta canaleta' posteriorly to the pore plate and depicted for *Am. nucula* (Balech, 1971). Another feature found in *Azadinium* and in *Am. languida* is a ventral pore (Tillmann *et al.*, 2012; Tillmann & Akselman, 2016). This is a hole, which is distinctly larger than normal thecal pores and forms within a platelet-like structure, and has different and species-specific positions on the ventral part of the epitheca. However, *Amphidoma parvula* is the first of the amphidomatacean species lacking this ventral pore, based on investigation using a contemporary, high resolution SEM. It is impossible to evaluate the presence/absence of a ventral pore for the older species of *Amphidoma* from the light microscopy-based older descriptions. Even when using SEM, Dodge & Saunders (1985) failed to detect the ventral pore in *Az. caudatum*, but it has been clearly identified recently (Nézan *et al.*, 2012).

The presence of a 'ventral pore' has been reported also for a few of the older *Amphidoma* species such as *Am. nucula*. Kofoid (1907*b*) depicted (but did not describe) a 'ventral pore' on his drawing, located mid-ventrally and slightly above the cingulum at the posterior tip of the first apical plate. In the same position (i.e. at the mid-ventral posterior tip of apical plate 1'), a 'ventral pore' was also described by Kofoid & Michener (1911) for *Am. laticincta*. The same structure, potentially, was noted by Balech (1971) in his detailed study of *Am. nucula*, in which he regarded *Am. spinosa* as synonym of *Am. nucula*. In his drawing there is a round, funnel-shaped structure at the proximal part of the Sa plate, which he described as a 'head shaped end'. We suggest that this structure (Balech: 'head shaped end of Sa', Kofoid: 'ventral pore') corresponds to the 'ventral depression' reported here for *Am. parvula*, sp. nov. The same 'ventral depression' is present in *Am. languida* (Tillmann *et al.*, 2017*b*) and is clearly different from the ventral pore as defined and found previously for species of *Azadinium* and *Am. languida*. There is a report of a 'ventral pore' for *Am. elongata*, which is located at the 'right edge of apical 1'' (Kofoid & Michener, 1911). This different position might indicate that the authors here observed a 'true' ventral pore, but confirmatory SEM analysis is needed to resolve this confusion.

Amphidoma parvula was isolated from the western South Atlantic Ocean off the Argentinean shelf. The communities of planktonic dinophytes in this area were intensively studied by Enrique Balech (e.g. Balech, 1988) almost 50 years ago, but given its delicate nature and small size it is quite likely that *Am. parvula* was simply overlooked in the past. During our cruise in 2015, *Am. parvula* was rarely seen alive in the plankton samples, and only 1 of 50 isolated strains of *Azadinium*/*Amphidoma* obtained represented *Am. parvula* The species was also present in a spring bloom from 1991 from the same area, where it was a rare member of a very diverse community of Amphidomataceae (Tillmann & Akselman, unpublished). This community was dominated by bloom-concentrations of *Azadinium luciferelloides* Tillmann & Akselman (Tillmann & Akselman, 2016), but *Az. spinosum, Az. dalianense, Az. dexteroporum* and *Am. languida* were also recorded. Moreover, a few other as yet undescribed species of *Amphidoma* and *Azadinium* were also identified in the community in low numbers – these will be described in more detail elsewhere. The very few specimens of *Am. parvula* observed in that sample conform to the formal species description of the H-1E9 strain presented here, including the inconsistent presence of a ventral depression at the anterior tip of plate Sa (Tillmann & Akselman, unpublished).

None of the known azaspiracids were found in strain H-1E9 of *Am. parvula*. This is important to note because AZAs were detected in *Am. languida* (Krock *et al.*, 2012; Tillmann *et al.*, 2015; Tillmann *et al.*, 2017*b*), and this species was identified as the cause of AZA contamination in shellfish above the

EU regulatory limit in Spanish Andalusia (Tillmann *et al.*, 2017*b*). *Amphidoma languida* has as yet been the only species of *Amphidoma* available to test for the presence of AZAs. Our finding of non-toxigenic *Am. parvula* shows that within *Amphidoma* there are both toxigenic and non-toxigenic species, as is also the case within the genus *Azadinium* (Tillmann *et al.*, 2014*b*). However, more strains of *Am. parvula* need to be analysed for AZA production, as AZA-producing strains and non-toxigenic strains within the same species are known for *Azadinium* (Krock *et al.*, 2014; Tillmann *et al.*, 2015; Rossi *et al.*, 2017).

Acknowledgements

Thanks to the Captain and crew of the FS *Bernardo Houssay* for their assistance and support for the collection of field material. We are grateful to Nancy Kühne for help with DNA extraction and sequencing and to Wolfgang Drebing for running the azaspiracid analyses. This study was supported by the project bilateral MINCYT-DAAD (Ministerio de Ciencia, Tecnología e Innovación Productiva, Argentina, and Deutscher Akademischer Austauschdienst, Germany), code DA/13/04, Grant 57130105, and by the PACES research program of the Alfred Wegener Institute as part of the Helmholtz Foundation initiative in Earth and Environment.

Disclosure statement

No potential conflict of interest was reported by the authors.

Supplementary information

The following supplementary material is accessible via the Supplementary Content tab on the article's online page at https://doi.org/10.1080/09670262.2017.1346205.

Supplementary figs S1–S12. *Amphidoma parvula,* sp. nov. (strain H-1E9): Variations in plate pattern observed in culture. **Figs S1–S3**. Basic plate pattern, ut unusual shape/size of certain apical plates. **Fig. S1**. Plate 3′ unusually wide and plate 5′ unusually narrow. **Fig. S2**. Plate 5′ with aberrant shape, displaced, and almost without contact to the pore plate. **Fig. S3**. Plate 5′ with aberrant shape leading to plate 4′ and 6′ being in contact. **Figs S4–S12**. Variations in apical plate number. **Fig. S4**. Seven precingular plates, presumably by a subdivision of plate 5″. Note that plate 6′ is unusually wide. **Figs S5–S7**. Five apical plates. **Figs S8–S12**. Seven apical plates. Note that in **Fig. S9** there are just 5 precingular plates. Note that in **Figs S11, S12** the right part of the subdivided plate 5′ is not in contact to the pore plate. Scale bars: 2 μm.

Supplementary figs S13–S21. *Amphidoma parvula*, sp. nov. (strain H-1E9): Variations in plate pattern observed in culture. **Fig. S13**. Multiple subdivisions of epithecal plates. **Fig. S14**. Aberrant form of plate 6′ being in contact to the pore. **Fig. S15**. Basic plate pattern, but unusual shape/size of the precingular plate 5′. **Fig. S16**. Presence of 7 precingular plates. **Figs S17–S21**. Variation in hypothecal plate pattern. **Figs S17, S18**. Presence of 5 postcingular plates. **Figs S19, S20**. Presence of seven postcingular plates in antapical (**Fig. S19**) and dorsal (**Fig. S20**) view. **Fig. S21**. Multiple subdivision of antapical plates. Scale bars: 2 μm.

Supplementary table S1. Voucher list

Supplementary video SV1. *Amphidoma parvula*, sp. nov (strain H1E9): swimming mode, living cells

Author contributions

U. Tillmann: original concept, sampling, isolation, culturing, LM and SEM, taxonomy, drafting and editing manuscript; M. Gottschling: analysis of molecular data, taxonomy, editing manuscript; V. Guinder: logistical support for sampling and isolation; B. Krock: LC-MS/MS analysis of azaspiracids.

ORCID

Marc Gottschling http://orcid.org/0000-0002-4381-8051

References

Akselman, R. & Negri, R.M. (2012). Blooms of *Azadinium* cf. *spinosum* Elbrächter et Tillmann (Dinophyceae) in northern shelf waters of Argentina, Southwestern Atlantic. *Harmful Algae*, **19**: 30–38.

Akselman, R., Negri, R.M. & Cozzolino, E. (2014). *Azadinium* (Amphidomataceae, Dinophyceae) in the Southwest Atlantic: *in situ* and satellite observations. *Revista de Biología Marina y Oceanografía*, **49**: 511–526.

Balech, E. (1971). Microplancton del Atlántico ecuatorial oeste (Equalant I). *República Argentina, Armada Argentina Servico de Hidrografía Naval, Buenos Aires*, **654**: 1–103.

Balech, E. (1988). Los dinoflagellados del Atlántico sudoccidental. *Publicaciones Especiales Instituto Español de Oceanografia*, **1**: 1–310.

Dodge, J.D. & Saunders, R.D. (1985). An SEM study of *Amphidoma nucula* (Dinophyceae) and description of the thecal plates in *A. caudata*. *Archiv für Protistenkunde*, **129**: 89–99.

Halldal, P. (1953). Phytoplankton investigations from Weather Ship M in the Norwegian Sea, 1948–49. *Hvalrådets Skrifter*, **38**: 1–91.

Keller, M.D., Selvin, R.C., Claus, W. & Guillard, R.R.L. (1987). Media for the culture of oceanic ultraphytoplankton. *Journal of Phycology*, **23**: 633–638.

Kofoid, C.A. (1907a). Dinoflagellates of the San Diego Region. III. Description of new species. *University of California Publications in Zoology*, **3**: 299–340.

Kofoid, C.A. (1907b). Reports on the scientific results of the expedition to the eastern tropical Pacific, in charge of Alexander Aggassiz, by the U.S. Fish Commission steamer 'Albatross', from October, 1904, to March, 1905, Lieut.-Commander L.M. Garrett, U.S.N., commanding. IX. New species of dinoflagellates. *Bulletin of the Museum of Comparative Zoology at Harvard College*, **50**: 163–207.

Kofoid, C.A. & Michener, J.R. (1911). Reports on the scientific results of the expedition to the eastern tropical Pacific, in charge of Alexander Agassiz, by the U.S. Fish Commission steamer 'Albatross', from October 1904, to

March, 1906, Lieut. L.M. Garrett, U.S.N., commanding. XXII. New genera and species of dinoflagellates. *Bulletin of the Museum of Comparative Zoology at Harvard College*, **54**: 267–302.

Krock, B., Tillmann, U., Voß, D., Koch, B.P., Salas, R., Witt, M., Potvin, E. & Jeong, H.J. (2012). New azaspiracids in Amphidomataceae (Dinophyceae): proposed structures. *Toxicon*, **60**: 830–839.

Krock, B., Tillmann, U., Witt, M. & Gu, H. (2014). Azaspiracid variability of *Azadinium poporum* (Dinophyceae) from the China Sea. *Harmful Algae*, **36**: 22–28.

Loeblich Jr, A.R. & Loeblich III, A.R. (1966). Index to the genera, subgenera, and sections of the Pyrrhophyta. *Studies in Tropical Oceanography*, **3**: 1–94.

Nézan, E., Tillmann, U., Bilien, G., Boulben, S., Chèze, K., Zentz, F., Salas, R. & Chomérat, N. (2012). Taxonomic revision of the dinoflagellate *Amphidoma caudata*: transfer to the genus *Azadinium* (Dinophyceae) and proposal of two varieties, based on morphological and molecular phylogenetic analyses. *Journal of Phycology*, **48**: 925–939.

Rossi, R., Dell'Aversano, C., Krock, B., Ciminiello, P., Percopo, I., Tillmann, U., Soprano, V. & Zingone, A. (2017). Mediterranean *Azadinium dexteroporum* (Dinophyceae) produces AZA-35 and six novel azaspiracids: a structural study by a multi-platform mass spectrometry approach. *Analytical and Bioanalytical Chemistry*, **409**: 1121–1134.

Schiller, J. (1929). Über eine biologische und hydrographische Untersuchung des Oberflächenwassers im westlichen Mittelmeer. *Botanisches Archiv*, **27**: 381–419.

Schiller, J. (ed.) (1937). *Dinoflagellatae (Peridineae) in monographischer Behandlung*. Dr. L. Rabenhorst's Kryptogamen-Flora von Deutschland, Österreich und der Schweiz Bd. 10 (3), Teil 2: 1–590 p. Johnson, New York.

Stein, F. (1883). *Der Organismus der Infusionsthiere nach eigenen Forschungen in systematischer Reihenfolge bearbeitet. III. Abt. II. Hälfte. Die Naturgeschichte der Arthrodelen Flagellaten*. W. Engelmann, Leipzig.

Tillmann, U. & Akselman, R. (2016). Revisiting the 1991 algal bloom in shelf waters off Argentina: *Azadinium luciferelloides* sp. nov. (Amphidomataceae, Dinophyceae) as the causative species in a diverse community of other amphidomataceans. *Phycological Research*, **64**: 160–175.

Tillmann, U., Elbrächter, M., John, U. & Krock, B. (2011). A new non-toxic species in the dinoflagellate genus *Azadinium: A. poporum* sp. nov. *European Journal of Phycology*, **46**: 74–87.

Tillmann, U., Elbrächter, M., Krock, B., John, U. & Cembella, A. (2009). *Azadinium spinosum* gen. et sp. nov. (Dinophyceae) identified as a primary producer of azaspiracid toxins. *European Journal of Phycology*, **44**: 63–79.

Tillmann, U., Gottschling, M., Nézan, E. & Krock, B. (2015). First record of *Azadinium dexteroporum* and *Amphidoma languida* (Amphidomataceae, Dinophyceae) from the Irminger Sea off Iceland. *Marine Biodiversity Records*, **8**: 1–11.

Tillmann, U., Gottschling, M., Nézan, E., Krock, B. & Bilien, G. (2014a). Morphological and molecular characterization of three new *Azadinium* species (Amphidomataceae, Dinophyceae) from the Irminger Sea. *Protist*, **165**: 417–444.

Tillmann, U., Jaen, D., Fernandez, L., Gottschling, M., Witt, M., Blanco, J. & Krock, B. (2017b). *Amphidoma languida* (Amphidomatacea, Dinophyceae) with a novel azaspiracid toxin profile identified as the cause of molluscan contamination at the Atlantic coast of southern Spain. *Harmful Algae*, **62**: 113–126.

Tillmann, U., Salas, R., Gottschling, M., Krock, B., O'Driscoll, D. & Elbrächter, M. (2012). *Amphidoma languida* sp. nov. (Dinophyceae) reveals a close relationship between *Amphidoma* and *Azadinium*. *Protist*, **163**: 701–719.

Tillmann, U., Salas, R., Jauffrais, T., Hess, P. & Silke, J. (2014b). AZA: the producing organisms – biology and trophic transfer. In *Seafood and Freshwater Toxins* (Botana, L.M., editor), 773–798. CRC Press, Boca Raton, FL.

Tillmann, U., Trefault, N., Krock, B., Parada-Pozo, G., De la Iglesia, R. & Vásquez, M. (2017a). Identification of *Azadinium poporum* (Dinophyceae) in the Southeast Pacific: morphology, molecular phylogeny, and azaspiracid profile characterization. *Journal of Plankton Research*, **39**: 350–367.